

The Disc-Jet Connection

Ralph E. Pudritz and Robi Banerjee

Department of Physics & Astronomy, McMaster University, Hamilton, ON L8S 4M1, Canada
emails: pudritz@physics.mcmaster.ca; banerjee@physics.mcmaster.ca

Abstract.

A large body of theoretical and computational work shows that jets - modelled as magnetized disk winds - exert an external torque on their underlying disks that can efficiently remove angular momentum and act as major drivers of disk accretion. These predictions have recently been confirmed in direct HST measurements of the jet rotation and angular momentum transport in low mass protostellar systems. We review the theory of disc winds and show that their physics is universal and scales to jets from both low and high mass star forming regions. This explains the observed properties of outflows in massive star forming regions, before the central massive star generates an ultracompact HII region. We also discuss the recent numerical studies on the formation of massive accretion disks and outflows through gravitational collapse, including our own work on 3D Adaptive Mesh simulations (using the FLASH code) of the hydromagnetic collapse of an initial rotating, and cooling Bonner-Ebert sphere. Magnetized collapse gives rise to outflows. Our own simulations show that both a jet-like disk wind on sub AU scales, and a larger scale molecular outflow occur (Banerjee & Pudritz 2005).

Keywords. bipolar outflows, jets, accretion discs, gravitational collapse

1. Introduction

The formation of massive stars is one of the most important areas of star formation research because of its broad implications for many different aspects of astrophysics - from the role that the first stars played in ending the cosmic dark age to the control that massive stars exert on galactic evolution. Of the two current theoretical models for the formation of massive stars - agglomeration through stellar collisions (eg. Bonnell et al. 1998) or accretion through a disk (eg. Yorke and Sonnalter 2002), the very earliest stages in the latter picture is a scaled up version of star formation as it is observed for lower mass stars.

In the accretion picture, most of the collapsing material in a massive and probably turbulent core forms a disk through which high disk accretion rates quickly assemble a massive star. In this early phase, and before an intense stellar radiation field turns on, it is natural to expect that jets and outflows will be driven from massive, magnetized disks (Blandford and Payne 1982, Pudritz and Norman 1983). These flows would be expected to be governed by the same physical principles as their low mass, TTS counterparts, and should pre-date the appearance of the compact HII region. We review the observational, theoretical, and computational basis for understanding the bipolar outflows in massive star forming regions in the following sections.

2. Observational clues - low vs high mass outflows and jets

Measurements of the thrust associated with molecular outflows provide an important body of evidence that low and high mass outflows have a common origin. One finds that CO outflows span nearly 5 decades in thrust F (units $10^{-4}M_{\odot}km/s yr^{-1}$) and have

orders of magnitude more thrust than can be accounted for by thermal or radiative drives. While there is a broad scatter, there is a clear relation between thrust and bolometric luminosity of the central source (Cabrit & Bertout, 1992);

$$F_{outflow}/F_{rad} = 250(L_{bol}/10^3L_{\odot})^{-0.3}. \quad (2.1)$$

This has been confirmed by the analysis of data from over 390 outflows, ranging up to 10^6L_{\odot} in central luminosity (Wu et al 2004).

CO outflows in regions of high mass star formation were first studied by Shepherd & Churchwell (1996). High resolution observations have since determined the collimation factors of these outflows which can be as high as 10, suggesting that these are true bipolar outflows and resemble those seen in low mass systems (eg. Beuther et al 2002). There are also a few clearcut cases of hot cores that have no centimeter-wave radio transmission yet which have massive outflows. Clearly, bipolar outflow precedes the appearance of an ultracompact HII region (Gibb et al 2004).

CO outflows in low mass systems are generally thought to trace the interaction between an underlying jet and the surrounding molecular gas (eg. reviews Cabrit et al 1997, Richer et al 2000). The coupling between the jet and the outflow has been modelled in two different ways: either as a jet-driven bow-shock (eg. Raga & Cabrit 1993, Masson & Chernin 1003) or as a wide-angle, X-wind driven shell (see review Shu et al. 2000). The observations for low mass systems suggest that both types of interaction may occur depending upon the source (Lee et al. 2000).

Discs in massive star forming regions are difficult to detect, but are present in at least some massive systems as early high spatial resolution observations showed (eg. Cesaroni et al. 1997, Zhang et al. 1998). One of the most interesting recent cases is the disk in the Omega Nebula (M17) wherein a flared disk of up to $M_{disc} \simeq 100M_{\odot}$ may be present (Chini et al. 2004).

What drives these outflows? While jets are still very difficult to detect in high mass outflows, direct observations of jet dynamics and jet-disc coupling have occurred for low mass systems. There are now two strong lines of observational evidence that support the theory that jets are collimated disc winds: (i) jet rotation and (ii) link between disk accretion and outflow.

High spatial and spectral resolution HST observations of emission line profiles of jets such as DG Tau clearly show line asymmetries on either side of the jet axis (eg. Bacciotti et al. 2002, Coffey et al. 2004). These can be interpreted as arising from the rotation of jets at $0.5''$ (or 110 AU) from the axis, at a speed of 6-15 km per sec. This rotation speed cannot arise from the innermost regions of the disk as predicted by X-wind models - the rotation speed would be much higher than observed in that case. Detailed fits (eg. Anderson et al. 2003) argue instead that the rotating material arises from an extended region of the disk ranging from 0.3 - 4.0 AU from the central star.

The link between disc accretion and mass outflow is well documented in many observational studies (Hartmann & Calvet 1995; review, Calvet 2003). For TTS, whether the system is accreting at a low rate of $\dot{M}_a \simeq 10^{-8}M_{\odot}yr^{-1}$, or in the FU Ori outburst state wherein $\dot{M}_a \simeq 10^{-4}M_{\odot}yr^{-1}$, the ratio of wind mass loss rate to disc accretion remains the same at about $\dot{M}_w/\dot{M}_a \simeq 0.1$. This disc-jet connection was predicted in early models of disc winds, and shown to be a direct consequence of the angular momentum equation and the efficiency of a magnetized wind to extract angular momentum from the disc. We turn to these ideas next.

3. Theory of disc winds - universal scaling

We consider the simplest possible description of a magnetized, rotating, object threaded by a large-scale field (see reviews; Königl & Pudritz 2000 (KP), Pudritz 2003). The equations of stationary, ideal MHD are the conservation of mass (continuity equation); the equation of motion with conducting gas of density ρ undergoing gas pressure (p), gravitational (from the central object whose gravitational potential is ϕ), as well as the Lorentz forces (from the field \mathbf{B}); the induction equation for the evolution of the magnetic field in the moving fluid; as well as the conservation of magnetic flux. These equations were written down by Chandrasekhar, Mestel, and many others.

One of the most interesting insights into the physics of magnetized outflows comes by from the conservation of mass and magnetic flux along a field line. Combining these, one can define a function k that is a constant along a magnetic field line and that we call the “mass load” of the wind;

$$\rho \mathbf{v}_{\mathbf{p}} = k \mathbf{B}_{\mathbf{p}} \quad (3.1)$$

This function represents the mass load per unit time, per unit magnetic flux of the wind. Its value is preserved along each field line emanating from the rotor (a disk in this case) and its value is determined on the disk surface. It can be more revealingly written as

$$k = \frac{\rho v_p}{B_p} = \frac{d\dot{M}_w}{d\Phi} \quad (3.2)$$

The mass load profile (as a function of the launching point of the wind) is determined by the physics of the underlying disc and plays an important boundary condition for all aspects of jet physics.

The toroidal field in rotating flows follows from the induction equation;

$$B_\phi = \frac{\rho}{k}(v_\phi - \Omega_o r). \quad (3.3)$$

where Ω_o is the angular velocity of the disk at mid-plane. This result shows that the strength of the toroidal field in the jet depends on the mass loading as well as the jet density. At high densities, one expects a stronger toroidal field. However, higher mass loads imply lower toroidal field strengths. Jet collimation depends on hoop stress through the toroidal field and because of this, the mass load has a very important effect on jet collimation (Ouyed & Pudritz 1999).

The angular momentum per unit mass can be deduced from the condition of angular momentum conservation along each field line;

$$l = r v_\phi - \frac{r B_\phi}{4\pi k} = \text{const.} \quad (3.4)$$

The form for l reveals that the total angular momentum is carried by both the rotating gas (first term) as well by the twisted field (second term), the relative proportion being determined by the mass load.

The amount of angular momentum per unit mass that is transported along each field line is fixed by the position of the Alfvén point in the flow - where the poloidal flow speed reaches the Alfvén speed for the first time ($m_A = 1$). It is easy to show that the value of the specific angular momentum is;

$$l(a) = \Omega_o r_A^2 = (r_A/r_o)^2 l_o \quad (3.5)$$

For a field line starting at a point r_o on the rotor (disk in our case), the Alfvén radius is $r_A(r_o)$ and constitutes a lever arm for the flow. Clearly, angular momentum is being

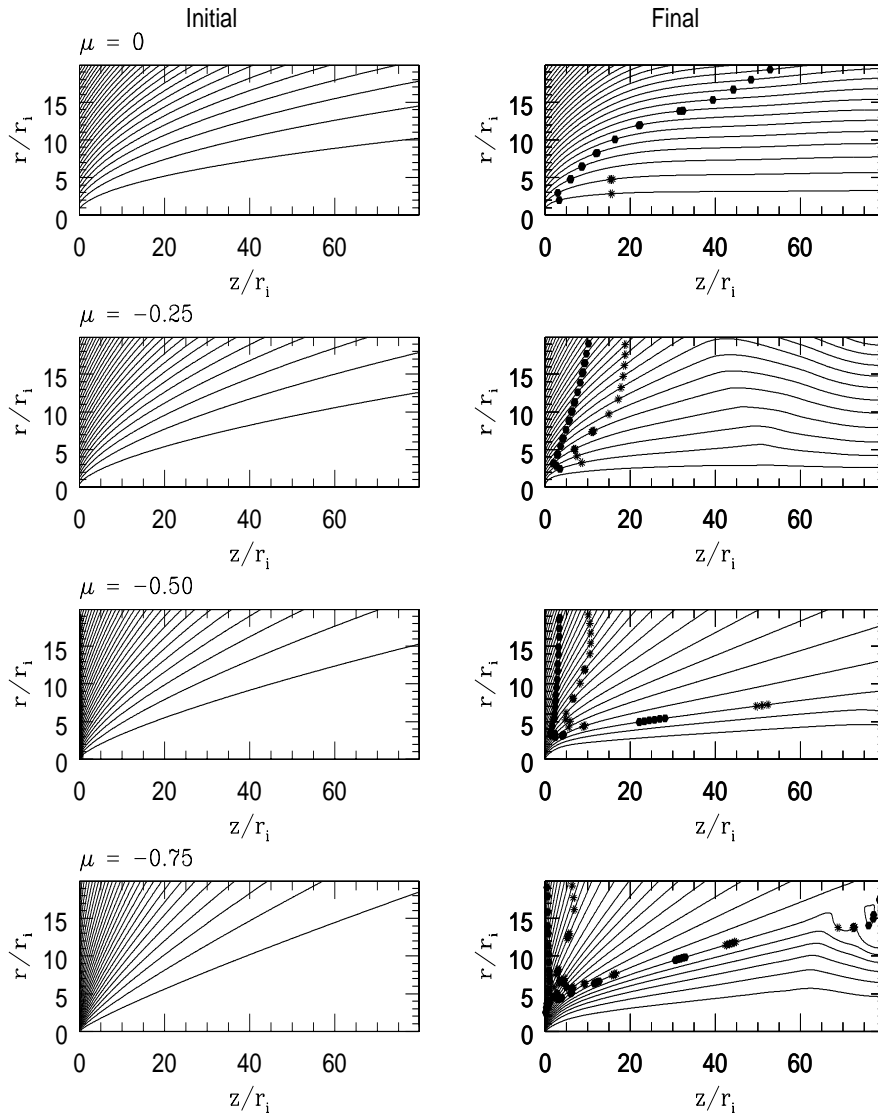


Figure 1. Initial (left panels) and final (right panels) magnetic configurations for disk winds for 4 models of the disc magnetic field. From top to bottom these are the potential solution, BP, PP, and a steeper $\mu = -0.75$ configuration (see equation 3.12). Outflows are less well collimated as one goes from top to bottom. (Adapted from PRO05).

extracted from the rotor such that the angular momentum per unit mass in the outflow is a factor of $(r_A/r_o)^2$ greater than it is for gas particles in the disk (l_o).

The terminal speed $v_p = v_\infty$ is such that the gravitational potential and rotational energy of the flow are negligible. For cold flows, the pressure may also be ignored. It follows that

$$v_\infty \simeq 2^{1/2} \Omega_o r_A = (r_A/r_o) v_{esc,o}. \quad (3.6)$$

We see that the terminal speed depends on the depth of the local gravitational well at the footpoint of the flow, and is therefore scalable.

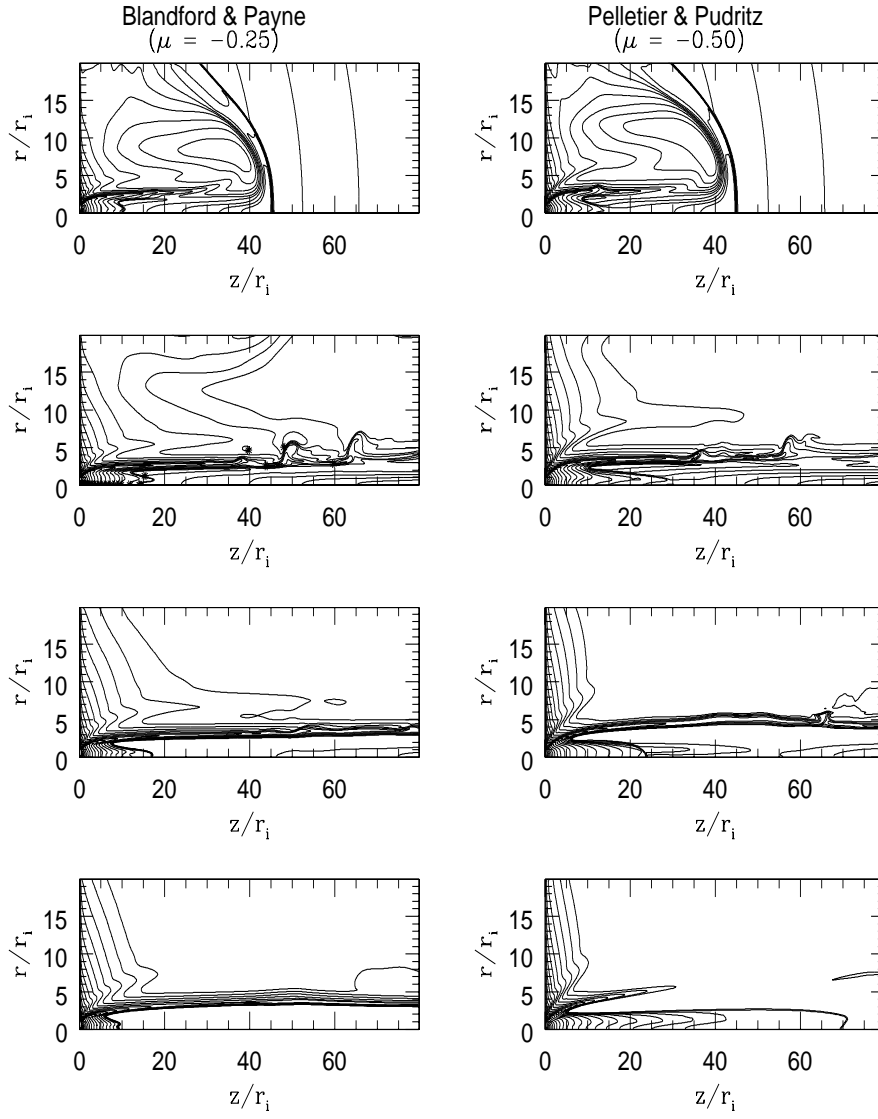


Figure 2. Four snapshots of the density structure of two jets shown in Figure 1: Blandford & Payne (left panels) vs. Pelletier & Pudritz (right panels). The jet density peaks for material moving close to the axis.

The angular momentum equation for the accretion disk undergoing an external magnetic torque may be written:

$$\dot{M}_a \frac{d(r_o v_o)}{dr_o} = -r_o^2 B_\phi B_z |_{r_o, H}. \quad (3.7)$$

This result shows that angular momentum is extracted from disks threaded by magnetic fields.

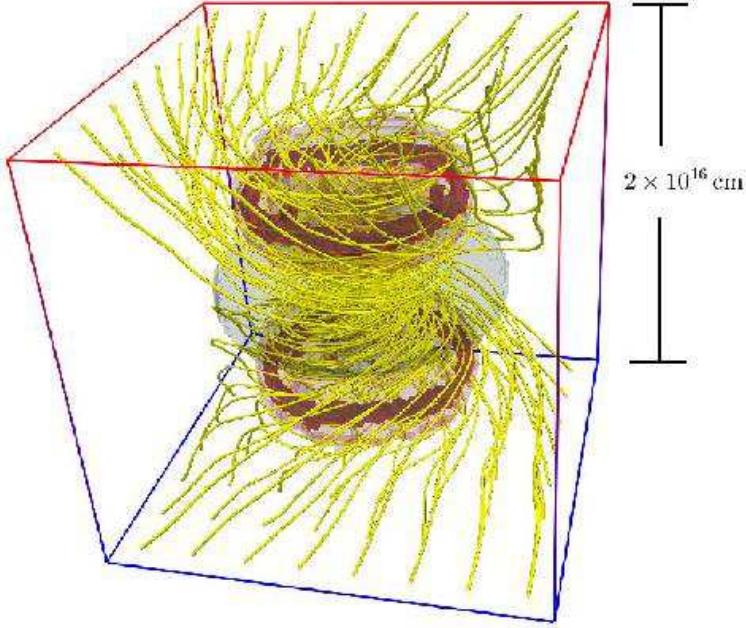


Figure 3. Magnetic field line structure of large-scale outflow from disc. Isosurfaces refer to velocities 0.2 and 0.4 km s⁻¹. (Adapted from BP05).

This equation can be cast into its most fundamental form;

$$\dot{M}_a \frac{d(\Omega_o r_o^2)}{dr_o} = \frac{d\dot{M}_w}{dr_o} \Omega_o r_A^2 (1 - (r_o/r_A)^2) \quad (3.8)$$

which reveals that there is a crucial link between the mass outflow in the wind, and the mass accretion rate through the disk. In order of magnitude, this is

$$\dot{M}_a = (r_A/r_o)^2 \dot{M}_w \quad (3.9)$$

The value of the Alfvén lever arm $r_A/r_o \simeq 3$ for most theoretical and numerical models that we are aware of, so that one finds $\dot{M}_w/\dot{M}_a \simeq 0.1$. Observations of DG Tau suggest that $r_A/r_o \simeq 1.8 - 2.6$ (Anderson et al 2003).

We may now connect this theoretical analysis with the observations of momentum and energy transport in the molecular outflows reviewed in §2. The total mechanical energy that is carried by the jet may be written as;

$$L_w = \frac{1}{2} \int_{r_i}^{r_j} d\dot{M}_w v_\infty^2 \simeq \frac{1}{2} \frac{GM_* \dot{M}_a}{r_i} [1 - (r_i/r_j)^2] \simeq \frac{1}{2} L_{acc}. \quad (3.10)$$

This results states that the wind luminosity taps the gravitational energy release through accretion in the gravitational potential of the central object.

We may also calculate the total momentum flux (thrust) carried by a jet launched from an accretion disk. For simplicity, assume that the Alfvén radius of flow along a field line whose footpoint is located at r_o obeys a power law scaling $r_A(r_o)/r_o \propto r_o^{-\alpha}$. The

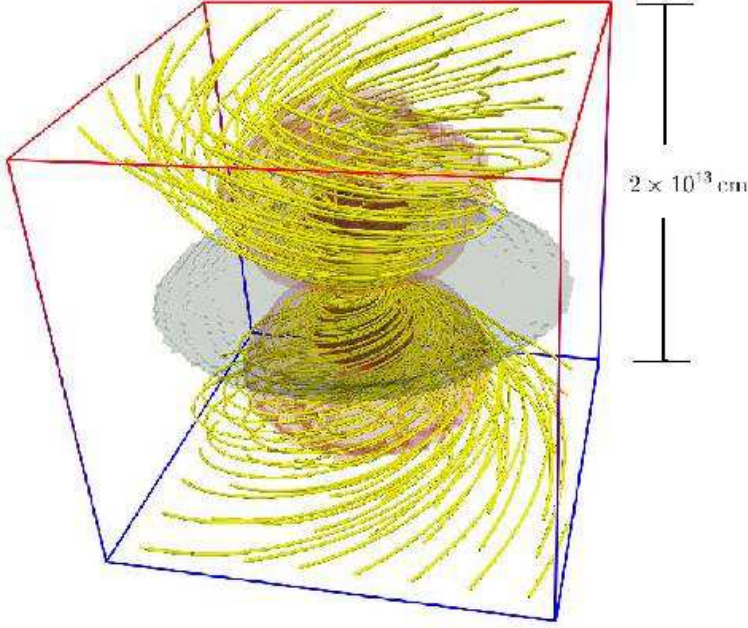


Figure 4. Magnetic field line structure of small-scale jet from disc. Isosurfaces refer to velocities 0.6 and 2 km s⁻¹. (Adapted from BP05).

thrust is then

$$F_w = \int_{r_i}^{r_j} d\dot{M}_w v_\infty = [f(\alpha)/2] \frac{r_i}{r_{A,i}} \dot{M}_a v_{esc,i} \quad (3.11)$$

where $f(\alpha) \equiv [(1/2) + \alpha]^{-1}$ the index i denotes the inner disk radius, and $v_{esc,i}$ is the escape speed from r_i . Again, one sees that the thrust is almost as high as it could theoretically be, and scales again with the depth of the gravitational well at the inner edge of the accretion disk.

A hydromagnetic wind collimates because of the increasing toroidal magnetic field in the flow as it moves through its various critical points and away from the disk. Collimation is achieved by the tension force associated with the toroidal field which leads to a radially inwards directed component of the Lorentz force (or "z-pinch"); $F_{Lorentz,z} \simeq J_z B_\phi$ where $\mathbf{J} = (c/4\pi)\nabla \times \mathbf{B}$ is the current density. Heyvaerts and Norman (1989) show that two types of solution for jet collimation are present depending upon the asymptotic behaviour of the total current intensity $I = 2\pi \int_0^r J_z(r', z') dr' = (c/2)rB_\phi$. In the limit that $I \rightarrow 0$ as $r \rightarrow \infty$, then the field lines are paraboloids which fill space. On the other hand, if the current is finite in this limit, then the flow is collimated to cylinders. Given that the toroidal field in the jet depends on the mass load, we see that the character of the flow therefore depends upon the boundary conditions on the disk. The similarity of collimation factors of low and high mass outflows may suggest that the physics of mass loading may be similar in low and high mass accretion discs as well.

These results have been rigorously tested by simulations of jets from thin disks by many authors (see KP). In Figures 1 and 2, we show jet simulations from the surfaces of

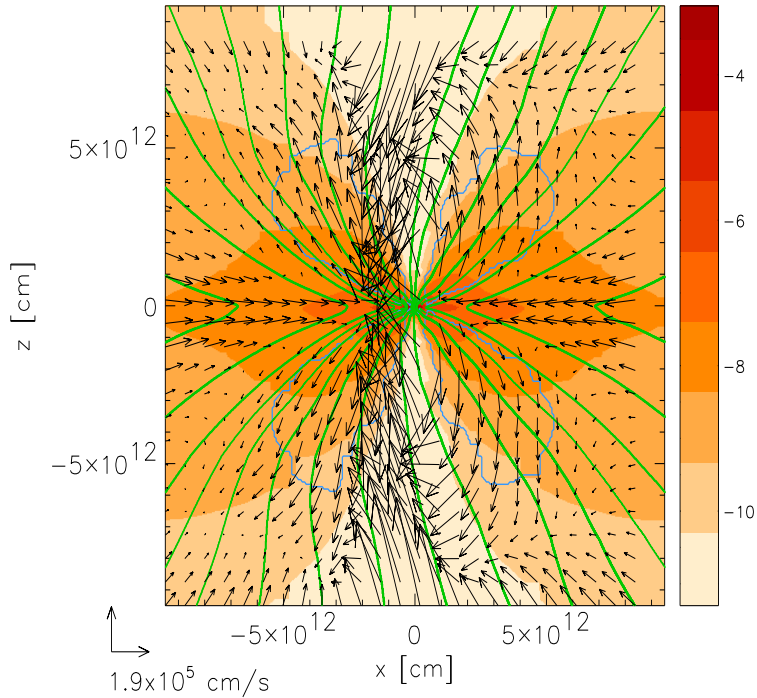


Figure 5. Cross section through the disc showing the launch of a centrifugally driven wind that impacts envelop material that is still infalling at this early time. (Adapted from BP05).

discs that are characterized by different mass load functions $k(r_o)$ across the disc surface (see Pudritz 2003, PRO 2005). We specify the surface $(r_o, 0)$ to have a power-law form $B_z(r_o, 0) = br_o^\mu$ and to exert no force on an initial corona, modelled as a gas with $\gamma = 5/3$. The solution for $\mu = 0$ is analytic and is the so-called "potential" configuration. Other values correspond to the BP model ($\mu = -1/4$), Pelletier & Pudritz (1992, PP92 ($\mu = -1/2$)), and a yet more steeply declining magnetic field such as $\mu = -3/4$. These initial configurations are plotted out in the left panels of Figure 1.

The injection speed v_{inj} of the material from the disk into the base of the corona - the injection speed - which is scaled with the local Keplerian velocity at each radius of the disk; $v_{inj} = 10^{-3}v_K$ at any point on the disk. Taken altogether, the mass loading at the footpoint of each field line on the disk takes the form;

$$k(r_o) = \rho_o v_{p,o} / B_{p,o} \propto r_o^{-3/2} r_o^{-1/2} / r_o^{-1+\mu} \propto r_o^{-1-\mu} \quad (3.12)$$

The right panels of Figure 1 show the final magnetic configurations. While the potential and BP cases achieve cylindrical collimation on the grid, the PP one is less well collimated while the last case presents a wide-angle wind. In Figure 2, we compare the density evolution at different times of the BP outflow (left) with the PP case. This Figure shows that the densest material in the jet does moves fairly parallel to the outflow axis. Figures 1 and 2 together show that disk winds can have both a wide-angle, as well as a cylindrically collimated aspect, depending upon the mass loading profile provided by the accretion disc, and is not a unique property of X-wind models alone. We see that one can have

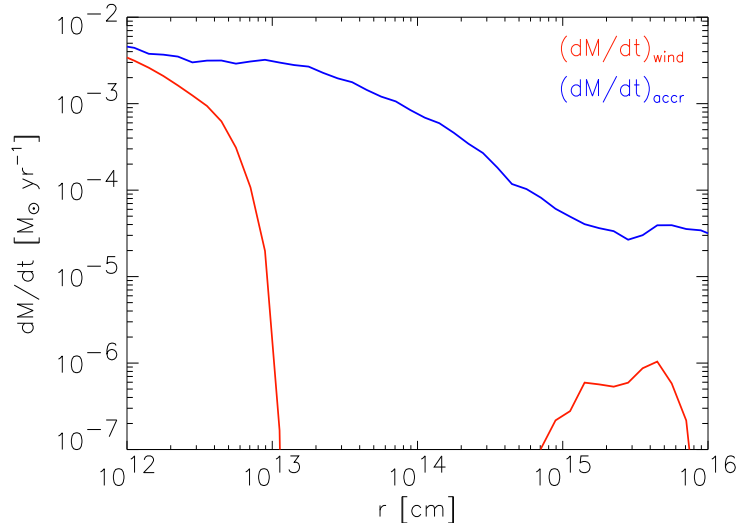


Figure 6. Accretion rate vs. mass loss rate in the outflow. (Adapted from BP05).

wide-angle, or cylindrically collimated flows that could explain the variety of observations noted in §2 (see PRO05 for details).

4. Outflow and jet formation during gravitational collapse

Outflows and jets are the earliest manifestations of star formation in both low and high mass systems. Therefore, they must arise in the early stages of gravitational collapse soon after the underlying accretion discs begin to form. What ingredients are necessary for outflow to occur?

Decades worth of purely hydrodynamical simulations of gravitational collapse in low mass systems have shown that outflows do not occur in such purely hydrodynamic collapse. The initial conditions for star formation have become much better defined with time. As an example, there are now excellent observations of low mass hydrodynamic cores that are very well fit by Bonner-Ebert density profiles (eg. Barnard 68 with $2.1 M_{\odot}$, Alves et al. 2001; B335 with $14 M_{\odot}$, Harvey et al. 2001).

We have recently carried out 3D simulations of the collapse of cooling, rotating low (Barnard 68) and high mass ($160 M_{\odot}$) B-E spheres (Banerjee et al 2004) using an Adaptive Mesh Refinement (FLASH) code. This allows us to resolve the local Jeans length in the system by as many as 12 pixels, with final results that resolves over 7 decades in length scale and can resolve down to 0.3 AU. Free-fall, isothermal collapse continues until the molecular cooling time is slower than the free-fall time - which occurs at a characteristic density of $10^{7.5} \text{ cm}^{-3}$. The gas undergoes a shock, and afterwards undergoes a second collapse onto the underlying disk. We observe that accretion through the disk is driven by a bar mode that manifests itself if the initial spin of the core obeys $\Omega t_{ff} \simeq 0.1$. For faster spin rates, the discs fragment into binary systems. Accretion rates through the discs in our high mass simulation reach peak values of $\simeq 10^{-3} M_{\odot} \text{ yr}^{-1}$.

Theoretical work over the last 2 decades has emphasized that magnetic fields are critical for the formation of outflows and jets. The first simulations of the collapse of magnetized cores and the onset of jets were produced by Tomisaka (1998). Using a nested grid scheme,

his calculations followed the collapse of a section of a magnetized cylinder and showed the onset of a large scale outflow and a jet on smaller scales (10 stellar radii typically).

Recently, we extended our purely hydrodynamic B-E collapse calculations to include a uniform, threading magnetic field. The change in dynamics is remarkable because we observe the onset of a large scale outflow on 100 AU scales as well an inner jet on sub AU scales (Banerjee & Pudritz 2005 (BP05)). In Figure 3 we show a 3D visualization of a large scale outflow that begins at about 70,000 yrs after the initiation of the collapse of the Barnard 68 low mass systems. It erupts from the surface of the disc at about 100 AU, and extends up to the outer accretion shock. By the end of the simulation it is still propagating outwards away from the disc driving a shock front ahead of it. It has the character of a slow, outward propagating magnetic tower that is driven by the gradient of the twisted toroidal field that is attached to the disc (Lynden-Bell 2003). This outflow is clearly dominated by a strongly wrapped toroidal field that pushes a ring of gas outwards and away from the disk.

The jet that arises on smaller scales is a true disc wind and it achieves super-Alfvénic speeds. It is shown in a 3D visualization in Figure 4, where we see the wrapped toroidal field lines that provide the collimating hoop stress on the jet. The jet has not yet burst out of the infall region. In Figure 5, we present an x-z plane section of the disc that is perpendicular to the disc midplane. The magnetic field lines in the disc are strongly bent away from the vertical axis by the accretion flow in the disc, which nicely sets up the initial condition for the centrifugal launch of the jet.

Finally, we show the mass transport rate in both the outflow (bottom, outer curve), and the inner jet (bottom, inner curve), as compared to the accretion rate. (top curve). These rates are computed as the average flow rate through a sphere of radius r . First, the accretion rate through these magnetized discs have increased compared to the pure hydrodynamic case. The accretion driven by the wind is comparable to the flow driven by the spiral waves in the disc at the point that our simulation ends. Second, the ratio of outflow to accretion rate through the inner part of the disc where the jet is active is $\dot{M}_w/\dot{M}_a \simeq 1/3!$

We conclude that jets and outflows are an intrinsic part of the collapse of magnetized cores, and that their properties are independent of the mass of the system. Both low and high mass outflows should share the same physics. Things change when the massive central star turns on its radiation field, but by that time, the outflow has already carved a channel through the core that may play a crucial part in relieving the radiation pressure in the interior region. This may promote the further growth, through accretion, of the central massive star (eg. Krumholz et al. 2005).

Acknowledgements

We thank Rachid Ouyed and Sean Matt for many interesting discussions on this topic. RB is a SHARCnet Fellow at McMaster University, and REP's research is supported by NSERC of Canada.

References

- Alves, J.F., Lada, C.J., Lada E.A. 2001, *Nature* 409, 159.
- Anderson, J.M., Li, Z.-Y., Krasnopolsky, R. & Blandford, R.D. 2003, *ApJ* 590, L107.
- Bacciotti, F., Ray, T.P., Mundt, R., Eilöffel, J., & Solf, J. 2002, *ApJ* 576, 222.
- Banerjee, R., Pudritz, R.E., & Holmes, L. 2004, *MNRAS* 355, 248.
- Banerjee, R., & Pudritz, R.E. 2005, *ApJ*, submitted.
- Beuther, H. et. al. 2002, *A & A* 387, 931.

- Blandford, R.D. & Payne, D.G. 1982, *MNRAS* 199, 883.
- Bonnell, H., Bate, M., & Zinnecker, H. 1998, *MNRAS* 298, 93.
- Cabrit, S. & Bertout, C. 1992, *A&A* 261, 274.
- Calvet, N. 2003, in: V. Beskin, G. Henri, F. Menard, G. Pelletier, & J. Dalibard (eds.) *NATO ASI: Accretion Discs, Jets, and High Energy Phenomena in Astrophysics*, p. 521.
- Cesaroni, R., Felli, M., Testi, L., Walmsley, C.M., & Olmi, L. 1997, *A&A* 325, 725.
- Chini, R. et al. 2004, *Nature* 429, 155.
- Coffey, D., Bacciotti, F., Woitas, J., Ray, T.P., & Eisloffel, J. 2004, *ApJ* 604, 758.
- Gibb, A.G., Wyrowski, F., & Mundy, L.G. 2004, *ApJ* 616, 301.
- Hartmann, L., & Calvet, N. 1995, *AJ* 109, 1846.
- Harvey, D.W.A., Wilner, D.J., Lada, C.J., Myers, P.C., Alves, J.F., & Chen, H. 2001, *ApJ* 563, 903.
- Heyvaerts, J., & Norman, C. A. 1989, *ApJ* 347, 1055.
- Königl, A., & Pudritz, R.E. 2000, in: V. Mannings, A.P. Boss, & S.S. Russell (eds.) *Protostars & Planets IV* (Tucson: Univ. of Arizona Press), p. 759.
- Krumholz, M.R., McKee, C.F., & Klein, R.I. 2005, *ApJ* 618, L33.
- Lee, C-F, Mundy, L.G., Reipurth, B., Ostriker, E.C., & Stone, J.M. 2000, *ApJ*, 542, 925.
- Lynden-Bell, D. 2003, *MNRAS* 341, 1360.
- Masson, C. R., & Chernin, L. M. 1993, *ApJ* 414, 230.
- Ouyed, R., Pudritz, R.E., & Stone, J.M. 1997, *Nature* 385, 409.
- Ouyed, R., & Pudritz, R.E. 1999, *MNRAS* 309, 233.
- Pelletier, G., & Pudritz, R.E. 1992, *ApJ* 394, 117.
- Pudritz, R.E., & Norman, C.A. 1983, *ApJ* 274, 677.
- Pudritz, R.E. 2003, in: V. Beskin, G. Henri, F. Menard, G. Pelletier, & J. Dalibard (eds.) *NATO ASI: Accretion Discs, Jets, and High Energy Phenomena in Astrophysics*, p. 187.
- Pudritz, R.E., Rogers, C.S., & Ouyed, R. 2005, *MNRAS*, submitted.
- Raga, A., & Cabrit, S. 1993, *A&A* 278, 267.
- Richer, J.S., Shepherd, D.S., Cabrit, S., Bachiller, R., & Churchwell, E. 2000, in: V. Mannings, A.P. Boss, & S.S. Russell (eds.) *Protostars & Planets IV* (Tucson: Univ. of Arizona Press), p. 867.
- Shepherd, D.S., & Churchwell, E. 1996, *ApJ* 472, 225.
- Shu, F. H., Najita, J., Shang, H., & Li, Z.-Y. 2000, in: V. Mannings, A. P. Boss, & S. S. Russell (eds.) *Protostars and Planets IV* (Tucson: Univ. Arizona Press), p. 789.
- Tomisaka, K. 1998, *ApJ* 502, L163.
- Wu, Y. et. al. 2004, *A&A* 426, 503.
- Yorke, H.W., & Sonnalter, C. 2002, *ApJ* 569, 846.
- Zhang, Q., Ho, P.T.P., & Ohashi, N. 1998, *ApJ* 494, 636.